MOLECULAR AND CELLULAR BIOLOGY, Nov. 2011, p. 4392–4404 Vol. 31, No. 22
0270-7306/11/$12.00 doi:10.1128/MCB.05517-11

Contribution of Casein Kinase 2 and Spleen Tyrosine Kinase to CFTR Trafficking and Protein Kinase A-Induced Activity▽‡

Simão Luz,[1]† Patthara Kongsuphol,[2]† Ana Isabel Mendes,[3] Francisco Romeiras,[1] Marisa Sousa,[1,3] Rainer Schreiber,[2] Paulo Matos,[3] Peter Jordan,[3] Anil Mehta,[4] Margarida D. Amaral,[1,3] Karl Kunzelmann,[2] and Carlos M. Farinha[1,3]*

University of Lisbon, Faculty of Sciences, BioFIG—Center for Biodiversity, Functional and Integrative Genomics, 1749-016 Lisbon, Portugal[1]; Department of Physiology, University of Regensburg, Regensburg, Germany[2]; Department of Genetics, National Institute of Health, Lisbon, Portugal[3]; and Division of Medical Sciences, University of Dundee, Ninewells Hospital, Dundee DD1 9SY, United Kingdom[4]

Received 19 April 2011/Returned for modification 3 June 2011/Accepted 13 September 2011

Previously, the pleiotropic "master kinase" casein kinase 2 (CK2) was shown to interact with CFTR, the protein responsible for cystic fibrosis (CF). Moreover, CK2 inhibition abolished CFTR conductance in cell-attached membrane patches, native epithelial ducts, and *Xenopus* oocytes. CFTR possesses two CK2 phosphorylation sites (S422 and T1471), with unclear impact on its processing and trafficking. Here, we investigated the effects of mutating these CK2 sites on CFTR abundance, maturation, and degradation coupled to effects on ion channel activity and surface expression. We report that CK2 inhibition significantly decreased processing of wild-type (wt) CFTR, with no effect on F508del CFTR. Eliminating phosphorylation at S422 and T1471 revealed antagonistic roles in CFTR trafficking: S422 activation versus T1471 inhibition, as evidenced by a severe trafficking defect for the T1471D mutant. Notably, mutation of Y512, a consensus sequence for the spleen tyrosine kinase (SYK) possibly acting in a CK2 context adjacent to the common CF-causing defect F508del, had a strong effect on both maturation and CFTR currents, allowing the identification of this kinase as a novel regulator of CFTR. These results reinforce the importance of CK2 and the S422 and T1471 residues for regulation of CFTR and uncover a novel regulation of CFTR by SYK, a recognized controller of inflammation.

Cystic fibrosis (CF) is the most common lethal genetic disease among Caucasians and is characterized by a chronic, destructive inflammatory lung disease as the major cause of mortality (5). CF is caused by mutations in the gene encoding the CF transmembrane conductance regulator (CFTR) protein, a polytopic integral membrane protein that functions as a cyclic AMP (cAMP)-activated chloride (Cl^-) channel and regulator of other channels at the apical membrane of epithelial cells (31). CFTR is a member of the ATP-binding cassette (ABC) transporter superfamily, and its structure includes two transmembrane domains (TMD1 and -2) that form the pore of the channel, two nucleotide binding domains (NBD1 and -2), and a regulatory domain (RD) containing several phosphorylation sites. Activation of CFTR occurs through binding of ATP and dimerization of the two NBDs, along with phosphorylation of the R domain by protein kinase A (PKA) at multiple phosphorylation sites (4, 22, 42).

CFTR is inserted cotranslationally into the endoplasmic reticulum (ER) membrane (17), where the ER quality control machinery targets a fraction of wild-type (wt) CFTR and almost all the protein bearing F508del (the most common mutation, present in about 70% of CF chromosomes) for degradation at the proteasome (15). F508del CFTR is partially functional when it is induced to traffic to the cell membrane (29, 35). The regulation of normal and mutant CFTR intracellular trafficking and activity is the result of a complex network of proteins which includes molecular chaperones (9, 10, 18), glycan-processing enzymes, and other transporters and channels (3) as well as the basal trafficking machinery (Rab GTPases, SNAREs, or PDZ domain proteins) (11, 28) and molecular switches (kinases and phosphatases). Together with PDZ domain-containing proteins, phosphorylation is involved in the formation of multiprotein signaling complexes that provide spatial and temporal specificity to CFTR function (14). However, its role in CFTR trafficking has so far remained unknown.

A previous study demonstrated that CK2 colocalized with wt CFTR in apical membranes of airway epithelial cells (39). It was found that inhibition of CK2 attenuates CFTR-dependent Cl^- transport in overexpressing cells, *Xenopus laevis* oocytes, and pancreatic ducts expressing wild-type CFTR. CK2 inhibition promptly closed CFTR Cl^- channels in cell-attached membrane patches and reduced the conductance of CFTR-expressing oocytes by about 80%. Moreover, coimmunoprecipitation suggested a direct interaction of wt CFTR but not of F508del CFTR with CK2. Interestingly, F508del CFTR Cl^- currents were insensitive to CK2 inhibitors, and a peptide mimicking the F508del region of CFTR failed to inhibit CFTR activity, whereas the wild-type peptide blocked CFTR function (39).

This early work hinted at a complexity of underlying protein-protein interactions involving CK2 and CFTR because no sig-

* Corresponding author. Mailing address: University of Lisbon, Faculty of Sciences, BioFIG—Center for Biodiversity, Functional and Integrative Genomics, 1749-016 Lisbon, Portugal. Phone: 351 921 750 09 32. Fax: 351 21 750 00 88. E-mail: cmfarinha@fc.ul.pt.
† S.L. and P.K. share first authorship.
▽ Published ahead of print on 19 September 2011.
‡ The authors have paid a fee to allow immediate free access to this article.

nificant inhibitory effect of pharmacological CK2 inhibition on CFTR function could be observed in excised patches of membranes detached from the very same cells that had just demonstrated prompt CFTR closure after 80 s of CK2 inhibition in the cell-attached mode (39). Subsequently, *in vitro* data suggested that a serine at position 422 within NBD1 was phosphorylated by CK2 with the surprising finding that the most likely candidate site at S511 near F508 was not labeled (26). Apart from this, there is only one preliminary report of another potential CK2 motif in the C-terminal end of CFTR (T1471) located within an acidic cluster (25).

Recent results point to a role for F508, S511, and nearby amino acids such as V510 in the allosteric control of the major structural forms of CK2 found in cells (27). These data are consistent with a model where the CFTR F508del peptide could bind different sites on isolated CK2alpha subunits than on the CK2(alpha/beta)$_2$ homodimer and suggest that CK2 targeting to subsets of its many targets may be perturbed in cells expressing F508del CFTR (27).

Interestingly, CFTR has a consensus for protein phosphorylation for spleen tyrosine kinase (SYK) at a nearby residue, i.e., Y512, consisting of a tyrosine followed by two negative residues (Y-E/D-E/D-X) (24). SYK is a cytosolic nonreceptor tyrosine kinase present in many cells, mainly involved in the regulation of the inflammatory process (30).

Since CK2 has been suggested to function as a multikinase anchor to CFTR, involving single protein kinases such as nucleoside diphosphate kinase (NDPK) and AMP-activated kinase (AMPK) (20), the proximity of Y512 with F508 and S511 may also account for an interplay of CK2 and SYK on CFTR traffic and function.

Because the roles of the different CK2 phosphorylation sites are poorly understood, we examined in detail their impact on maturation and Cl^- channel function of CFTR. Our data suggest an antagonistic role of residues S422 and T1471 in the regulation of CFTR function and trafficking by CK2. Our data confirm regulation of CFTR by SYK, which interacts with CFTR in the *in vivo* phosphorylating of NBD1 at Tyr512, but exclude any role for residue S511 in the functional interaction of CFTR and CK2 by using a number of CFTR mutants.

MATERIALS AND METHODS

Site-directed mutagenesis, cells, and CFTR expression. By using the QuikChange mutagenesis kit (Stratagene, La Jolla, CA), we introduced mutations into CFTR in the pNUT or the pBluescript vector (32, 37). BHK cells were transfected with 2 μg of each pNUT-CFTR variant by using Lipofectamine 2000 (Invitrogen, Carlsbad, CA) and selected for stable transfectants by using 500 μM methotrexate. After 10 days, individual clones were isolated and assessed for CFTR expression by Western blotting (WB).

Western blotting. WB was performed as described previously (10). Briefly, cells were lysed with sample buffer (1.5% [wt/vol] SDS, 5% [vol/vol] glycerol, 0.001% [wt/vol] bromophenol blue, 0.5 mM dithiothreitol [DTT], and 31.25 mM Tris, pH 6.8). Total protein was quantified by a modified micro-Lowry method, and 30 μg of total protein was loaded onto 7% (wt/vol) SDS-PAGE gels for electrophoretic separation and transferred onto polyvinylidene difluoride (PVDF) filters. The filters were probed with the anti-CFTR monoclonal antibody (MAb) 596 (CFF, Bethesda, MD) to detect specifically CFTR and the Super-Signal West Pico chemiluminescent substrate system (Pierce, Rockford, IL) to develop WB. As a loading control, blots were reprobed with the anti-α-actin Ab (Sigma). Films were digitalized on an ImageScanner (GE Healthcare). Integrated peak areas were determined using the gel analysis ImageQuant software (GE Healthcare).

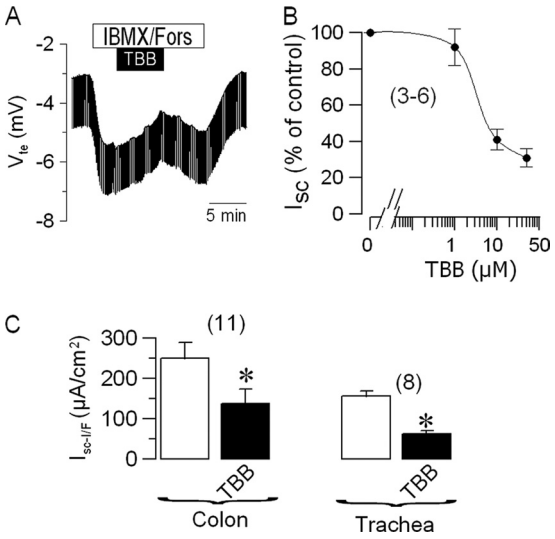

FIG. 1. Regulation of Cl^- transport in native epithelial cells by CK2. (A) Original Ussing chamber recording from a mouse colon measured under open-circuit conditions, showing the lumen-negative transepithelial voltage generated by the transport activity of the tissue. Stimulation of tissue by IBMX/forskolin (100 μM/2 μM, respectively) induced a negative voltage deflection due to activation of Cl^- secretion. Reversible inhibition of the Cl^- secretion by TBB (10 μM). (B) Dose-response curve for the inhibitory effects of TBB on IBMX (100 μM)- and forskolin (5 μM)-induced Cl^- secretion in excised mouse trachea as measured in Ussing chamber recordings. (C) Summary of the calculated equivalent short-circuit currents demonstrating inhibition of IBMX/forskolin-activated transport by TBB (10 μM) in both mouse colon and trachea. Data indicate means ± standard errors of the means. Numbers in parentheses are the numbers of experiments. Asterisks indicate significant inhibition by TBB (paired *t* test).

Pulse-chase and immunoprecipitation. Cells expressing CFTR were starved for 30 min in methionine-free medium and then pulsed for 30 min at 37°C in the same medium supplemented with 150 μCi [^{35}S]methionine. Pulse-chase experiments, followed by immunoprecipitation (IP) with an anti-CFTR MAb, were performed as previously described (10). Briefly, after chasing for 0, 0.5, 1, 2, and 3 h in regular medium with 5% (vol/vol) fetal bovine serum and 1 mM nonradioactive methionine, cells were lysed in 1 ml of RIPA buffer (1% [wt/vol] deoxycholic acid, 1% [vol/vol] Triton X-100, 0.1% [wt/vol] SDS, 50 mM Tris, pH 7.4, and 150 mM NaCl) and immunoprecipitation of CFTR was carried out with 1 μg of MAb 596 (CFF, Bethesda, MD) or MAb M3A7 (Chemicon) and protein G-agarose beads. Immunoprecipitated proteins were eluted for 1 h at room temperature in sample buffer (see above) and then electrophoretically separated by SDS-PAGE. SDS-PAGE, fluorography, densitometry, and statistical analysis were also performed as described previously (10). The number of cells used for labeling and immunoprecipitation experiments was 2×10^6 cells for each time point. Densitometry was performed as described above.

Coimmunoprecipitation. Cells were grown in 100-mm plates and lysed on ice in 1 ml nondenaturing lysis buffer (50 mM Tris-HCl, pH 7.5, 1% NP-40, 100 mM NaCl, 10% glycerol, 10 mM $MgCl_2$) supplemented with a protease inhibitor cocktail. The cell lysates were precleared with protein G-agarose beads for 1 h at 4°C, then incubated for 2 h at 4°C with either anti-SYK polyclonal Ab (PAb) (sc-929; Santa Cruz Biotechnology, Santa Cruz, CA) or anti-CFTR 596 MAb, then further incubated for 1 h with protein G-agarose beads (Roche Applied Science, Indianapolis, IN), and finally washed three times in cold lysis buffer containing 200 mM NaCl. Proteins were solubilized from the beads in 2× SDS sample buffer and separated by 10% SDS-polyacrylamide gel electrophoresis. WB was performed as described above with anti-SYK PAb.

***In vitro* phosphorylation.** For *in vitro* protein kinase assays, 1 μg of a recombinant fragment of human CFTR (amino acids corresponding to the first nucleotide binding domain, NBD1 [36]) was resuspended in 20 μl kinase reaction buffer (30 mM Tris-HCl, pH 7.5, 10% [vol/vol] glycerol, 1 mM DTT, 1 mM Na_3VO_4, 37.5 mM $MgCl_2$, and 250 μM ATP) and incubated in the presence of 5 mCi [γ-^{32}P]ATP at 30°C for 30 min with beads containing either immunopre-

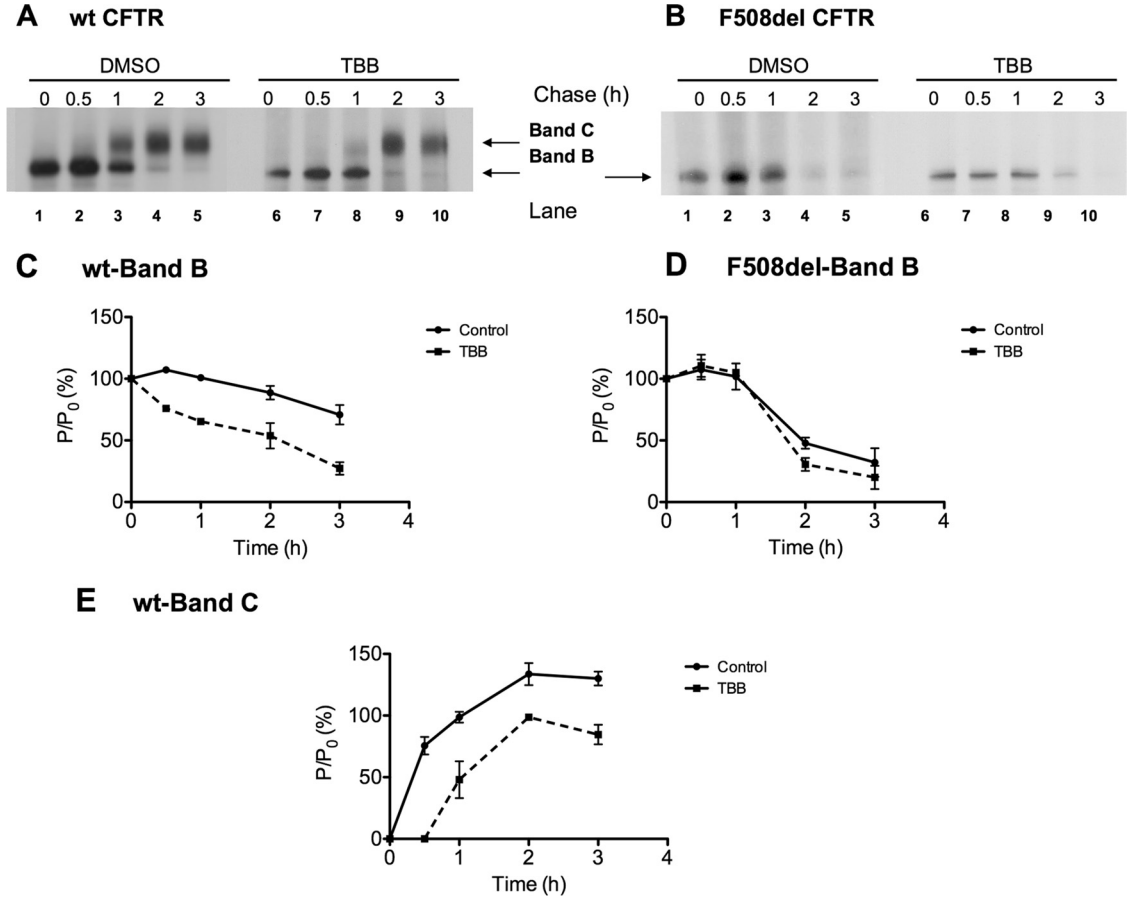

FIG. 2. Turnover and processing of wt and F508del CFTR under treatment with the CK2 inhibitor TBB. BHK cells stably expressing wt (A) or F508del (B) CFTR were treated for 90 min with 20 μM TBB or with the same volume percentage of dimethyl sulfoxide (DMSO) as a control. After preincubation with TBB, cells were pulse-labeled for 30 min with [^{35}S]methionine and chased for 0, 0.5, 1, 2, and 3 h. Cells were then lysed and immunoprecipitated with an anti-CFTR M3A7 Ab. Following electrophoretic separation and fluorography, immature (band B) and mature (band C) forms of CFTR were quantified with the ImageQuant software. Turnover of the core-glycosylated form (band B) of wt (C) and F508del (D) CFTR is shown as the ratio between P, the amount of band B at time *t*, and P_0, the amount of band B at the start of the chase (i.e., at the end of pulse). The efficiency of conversion of the core-glycosylated form (band B) into the fully glycosylated form of wt CFTR (band C) was also estimated for wt CFTR (E) and determined as band C at time *t* as a percentage of the amount of band B at the start of the chase (P_0). Images are representative of a total of three experiments.

cipitated green fluorescent protein (GFP) or yellow fluorescent protein (YFP)-SYK protein. Then, 5× Laemmli SDS sample buffer was added to the reaction mixtures and proteins were separated by SDS-PAGE followed by transfer to a PVDF membrane. The membrane was first analyzed by autoradiography followed by WB using the indicated antibodies.

Cell surface biotinylation. BHK cells stably expressing CFTR variants were washed twice with warm culture medium to remove dead cells and placed on ice in a cold room. Cells were washed three times with ice-cold PBS-CM (phosphate-buffered saline [PBS], pH 8.0, containing 0.1 mM $CaCl_2$ and 1 mM $MgCl_2$) and left for 5 min in cold PBS-CM to ensure arrest of endocytic traffic. Cells were then incubated for 30 min with 0.5 mg/ml EZ-Link sulfo-NHS-SS-biotin (Pierce Biotechnology, Rockford, IL; catalog no. 21331) in PBS-CM before being rinsed twice and left for 15 min on ice with ice-cold Tris-glycine (100 mM Tris-HCl, pH 8.0, 150 mM NaCl, 0.1 mM $CaCl_2$, 1 mM $MgCl_2$, 10 mM glycine, 1% bovine serum albumin [BSA]) to quench the biotinylation reaction. Cells were again washed three times with cold PBS-CM and lysed in 250 μl pulldown buffer (50 mM Tris-HCl, pH 7.5, 100 mM NaCl, 10% glycerol, 1% NP-40) in the presence of a protease inhibitor cocktail composed of 1 mM phenylmethylsulfonyl fluoride (PMSF), 1 mM 1,10-phenanthroline, 1 mM EGTA, 10 μM E64, and 10 μg/ml each of aprotinin, leupeptin, and pepstatin A (all from Sigma-Aldrich Quimica, Madrid, Spain). The cell lysates were harvested by scraping and cleared by centrifugation at 16,000 × *g* at 4°C for 5 min. An aliquot of 40 μl representing the total CFTR level was removed and added to 2× CFTR sample buffer (62.5 mM Tris-HCl, pH 6.8, 3% SDS, 10% glycerol, 0.02% bromophenol blue, 160 mM DTT), while 200 μl lysate was added to 25 μl streptavidin-agarose beads (Sigma-Aldrich) previously incubated for 1 h in 1 ml cold pulldown buffer containing 2% nonfat milk powder and washed three times in pulldown buffer. For purification of biotinylated proteins, lysate and beads were incubated under rotation for 1 h at 4°C and the beads were collected by centrifugation (1 min at 3,000 × *g*) and washed three times in cold wash buffer (100 mM Tris-HCl, pH 7.5, 300 mM NaCl, 1% Triton X-100). Captured proteins were recovered from the beads in 25 μl 2× CFTR sample buffer. The biotinylated protein fraction and whole-cell lysates were analyzed in parallel by SDS-PAGE followed by WB.

cRNA and DEVC. cRNA syntheses were performed based on *in vitro* transcription techniques, using T7, T3, or SP6 promoter and polymerase (Promega). *Xenopus laevis* oocytes were defolliculated by incubation at 18°C for 1 h with collagenase V (Sigma) in OR2 solution (82.5 mM NaCl, 2 mM KCl, 1 mM $MgCl_2$, and 5 mM HEPES, pH 7.55). Oocytes were injected with 10 ng cRNA (in a total volume of 47 nl) encoding wt, S422A, S422D, Y512A, Y512D, Y512F, T1471A, T1471D, F508del, F508del-S422A, F508del-S422D, F508del-Y512A, F508del-Y512D, F508del-Y512F, F508del-T1471A, or F508del-T1471D CFTR. Oocytes were incubated at 18°C for 2 to 4 days in ND97 solution (96 mM NaCl, 2 mM KCl, 1.8 mM $CaCl_2$, 1 mM $MgCl_2$, 5 mM HEPES, 2.5 mM sodium pyruvate, 0.5 mM theophylline, and 0.01 mg/ml gentamicin, pH 7.55) before subjection to double-electrode voltage clamp (DEVC). Whole-cell currents were measured by impaling the oocyte membrane with two electrodes (Clark Instru-

ments Ltd., Salisbury, United Kingdom) that were filled with 3 M KCl and had a resistance less than 1 MΩ. Membrane voltages were clamped (oocyte clamp amplifier; Warner Instruments LLC, Hamden, CT) from −60 to 40 mV. The bath was continuously perfused at a rate of 5 ml/min. The voltage drop across the serial resistance was adjusted to zero by two bath electrodes and a virtual-ground head stage. All experiments were conducted in ND96 solution (96 mM NaCl, 2 mM KCl, 1.8 mM $CaCl_2$, 1 mM $MgCl_2$, 5 mM HEPES, and 2.5 mM sodium pyruvate, pH 7.55) at room temperature (22°C).

Animals and Ussing chamber experiments. Animal studies were conducted according to the German laws on protection of animals. Mice (C57BL/6; Charles River, Germany) were sacrificed under CO_2 narcosis by cervical dislocation. Mouse tracheas were dissected, opened longitudinally on the opposite side of the cartilage-free zone, and transferred immediately into an ice-cold buffer solution. Stripped colon was put into an ice-cold bath solution (145 mM NaCl, 0.4 mM KH_2PO_4, 1.6 mM K_2HPO_4, 6 mM D-glucose, 1 mM $MgCl_2$, 1.3 mM calcium gluconate, pH 7.4) containing amiloride (10 μM) and indomethacin (10 μM). Experiments were performed as described previously (1). Briefly, after being mounted into a perfused micro-Ussing chamber, apical and basolateral surfaces of the epithelium were perfused continuously with buffer solution at a rate of 5 to 10 ml/min (chamber volume, 2 ml). All experiments were carried out at 37°C under open-circuit conditions. Transepithelial resistance (R_{te}) was determined by applying short (1-s) current pulses (I = 0.5 μA) and the corresponding changes in transepithelial voltage (V_{te}) and basal V_{te} were recorded continuously. Values for V_{te} were referred to the serosal side of the epithelium. The equivalent short-circuit current (I_{sc}) was calculated according to Ohm's law from V_{te} and R_{te} ($I_{sc} = V_{te}/R_{te}$).

Materials and statistical analysis. All compounds used were of the highest available grade of purity and were from Sigma (St. Louis, MO) or Calbiochem (San Diego, CA). The compounds used in this study were usually applied at recommended maximal concentrations to achieve full activation or inhibition. For statistical analysis, the Student t test was used to compare any two different groups. Differences in multiple groups were analyzed using one-way analysis of variance (ANOVA) followed by the Tukey test to compare significant differences between individual groups. P values of ≤0.05 were considered significant.

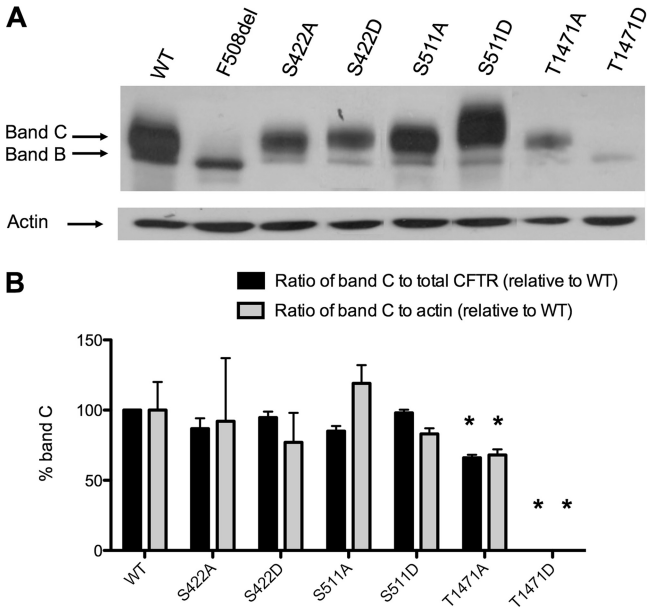

FIG. 3. Steady-state levels of CFTR bearing S422, S511, and T1471 mutations. (A) WB of total protein (30 μg) from BHK cells stably expressing CFTR bearing different mutations. Actin was also assessed as a loading control. (B) Processing of CFTR at steady state was assessed by densitometry and shown as the ratio of band C to total CFTR (C/B+C), normalized to wt CFTR (black bars). The amount of mature band C CFTR was also assessed as ratio of band C to actin, again normalized to wt CFTR (grey bars). Asterisks indicate significant differences from wt CFTR (t test, $P < 0.05$).

RESULTS

Regulation of CFTR by CK2 is important in mouse colonic and airway epithelia. Previous observations show that CK2-dependent regulation is observed not only in CFTR-overexpressing cells but also in excised epithelial tissues (25, 39). To test our hypothesis that CK2 is an important regulator of CFTR under physiological conditions, we extended these studies to native mouse epithelial tissues. We removed mouse distal colon and trachea from sacrificed animals and performed open-circuit Ussing chamber recordings. The lumen-negative transepithelial voltage was enhanced by stimulation of mouse colon with isobutylmethylxanthine (IBMX; 100 μM) and forskolin (Fors; 2 μM). Almost all the entire short-circuit current (I_{sc}) that was activated by IBMX and forskolin is CFTR, since 5 μM CFTRinh172 reduced IBMX/Fors (I/F)-activated I_{sc} from 248 ± 29 μA/cm^2 to 61 ± 19 μA/cm^2 (n = 4, colon) and from 158 ± 12 μA/cm^2 to 41 ± 13 μA/cm^2 (n = 5, trachea).

Application of the CK2 inhibitor TBB (4,5,6,7-tetrabromobenzotriazole; 10 μM) in the presence of IBMX/forskolin inhibited the transepithelial voltage reversibly, thus demonstrating inhibition of CFTR that had been previously activated by IBMX/forskolin (Fig. 1A). When calculating the equivalent short-circuit current (I_{sc}), we found significant inhibition of IBMX/forskolin-induced I_{sc} by TBB in both distal colonic and airway epithelium (Fig. 1C). Importantly, our earlier work demonstrated that TBB was highly selective for CK2 by showing that coexpression of a TBB-insensitive form of CK2 eliminated the ability of TBB to inhibit PKA-activated CFTR (39). In addition, we observed that the onset of the inhibition with TBB occurred at about 1 μM, a concentration that is highly specific for CK2 (Fig. 1B). Thus, these combined data indicate that CK2 is an important regulator of CFTR-dependent Cl^- transport in native epithelia and that TBB is a specific pharmacological agent for the further investigation of the role of CK2 in CFTR function. Inhibition of IBMX/Fors-activated I_{sc} by TBB was also confirmed using another CK2 inhibitor, quinalizarin (5 μM) (6). Application of quinalizarin reduced the I_{sc} by 81% ± 11% (n = 3; colon) and by 79% ± 16% (n = 3; trachea) (data not shown).

CFTR turnover and processing under CK2 inhibition. In order to define the role of CK2 in CFTR turnover and processing, we assessed the concomitant effects of the inhibition of the kinase by a pulse-chase approach. For this, cells were incubated for 90 min with the CK2 inhibitor TBB before performing pulse-chase and immunoprecipitation (IP) of CFTR and the experiments were performed still in the presence of the inhibitor. We also assessed cell viability to exclude any effect of incubation with TBB (data not shown).

The results in Fig. 2 show that 20 μM TBB both increases the turnover of immature wt CFTR (Fig. 2B) and decreases the efficiency of its processing into the mature glycosylated form (band C, Fig. 2A and dashed lines in Fig. 2C and E). This effect occurs despite the expected suppressive effects of CK2 inhibition of protein synthesis given that CK2 controls up to 75% of cell proliferation (compare left and right panels in Fig. 2A and B, normalized to starting abundance in Fig. 2C, D, and E). In contrast, CK2 inhibition by TBB does not produce any detectable effect upon the turnover of immature F508del CFTR (Fig. 2D). These results show that CK2 activity affects the stability of

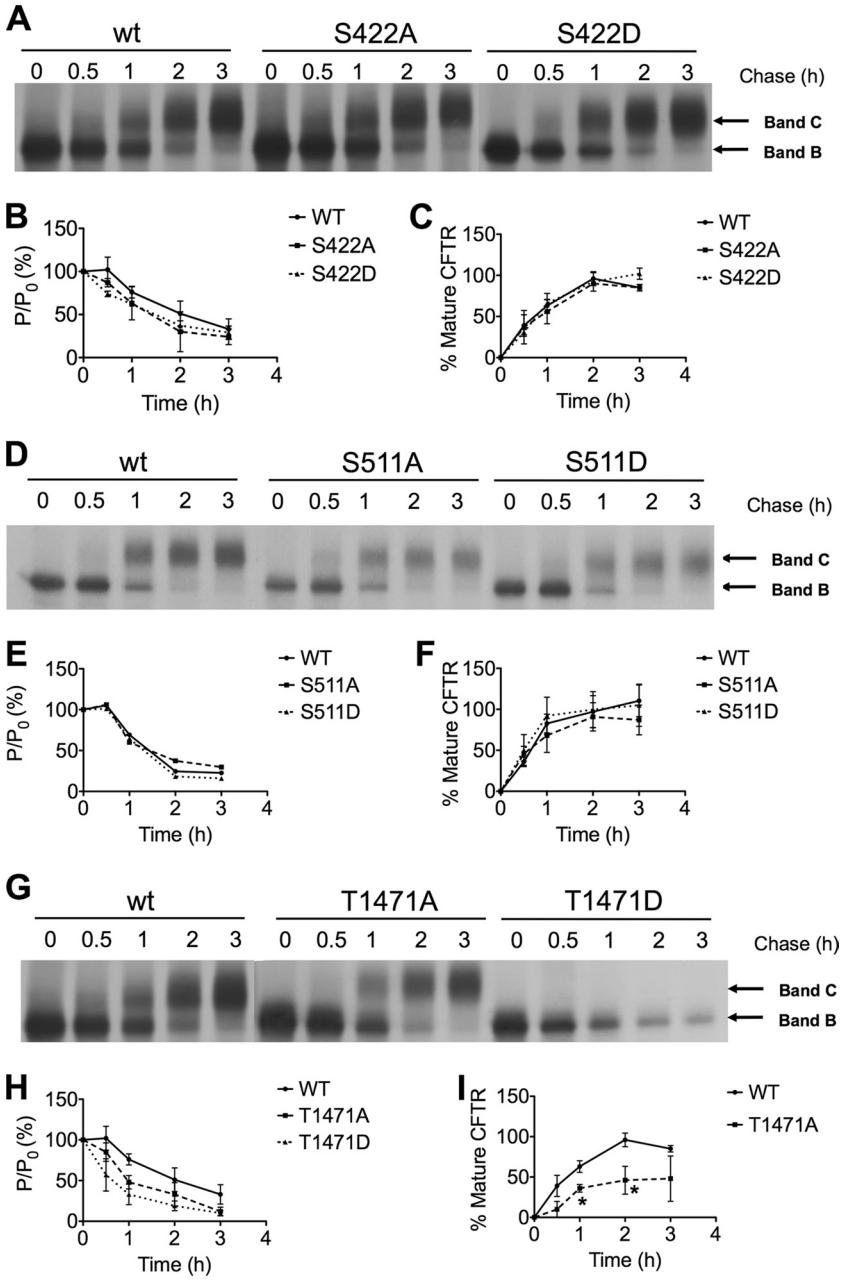

FIG. 4. Turnover and processing of CFTR bearing S422, S511, and T1471 mutations. BHK cells stably expressing S422A or S422D CFTR (A), S511A or S511D CFTR (D), and T1471A or T1471D CFTR (G) were analyzed by pulse-chase as in Fig. 2 followed by immunoprecipitation with anti-CFTR M3A7 or 596 antibodies. Electrophoresis, fluorography, and quantification were also performed as in Fig. 2. Turnover of the core-glycosylated form (band B) of S422A/D (B), S511A/D (E), and T1471A/D CFTR (H) is shown as the ratio between P, the amount of band B at time t, and P_0, the amount of band B at the start of the chase (i.e., at the end of pulse). The efficiency of conversion of the core-glycosylated form (band B) into the fully glycosylated form of wt CFTR (band C) was also estimated for S422A/D (C), S511A/D (F), and T1471A/D CFTR (I) and determined as the percentage of band C at time t relative to the amount of band B at the start of the chase (P_0). Images and quantitations are representative of a total of 3 to 4 experiments. Asterisks in panel I indicate differences from wt CFTR for the time points indicated (t test, $P < 0.05$).

the immature form of wt CFTR (but not F508del CFTR) and its trafficking through the Golgi complex, here detected by the delayed and attenuated appearance of its fully glycosylated form (Fig. 2E). Thus, these data suggest that TBB reduces band B stability, accelerates its destruction, and delays band C appearance by around 30 min (Fig. 2A, C, and E, respectively).

Mutation of consensus CFTR sites for CK2 phosphorylation. Since we found that CK2 inhibition affects wt CFTR processing, our next aim was to investigate the molecular mechanism of this effect. To this end, we screened CFTR sequence both manually and using NetPhosK1.0 phosphorylation site prediction software (2) so as to identify potential

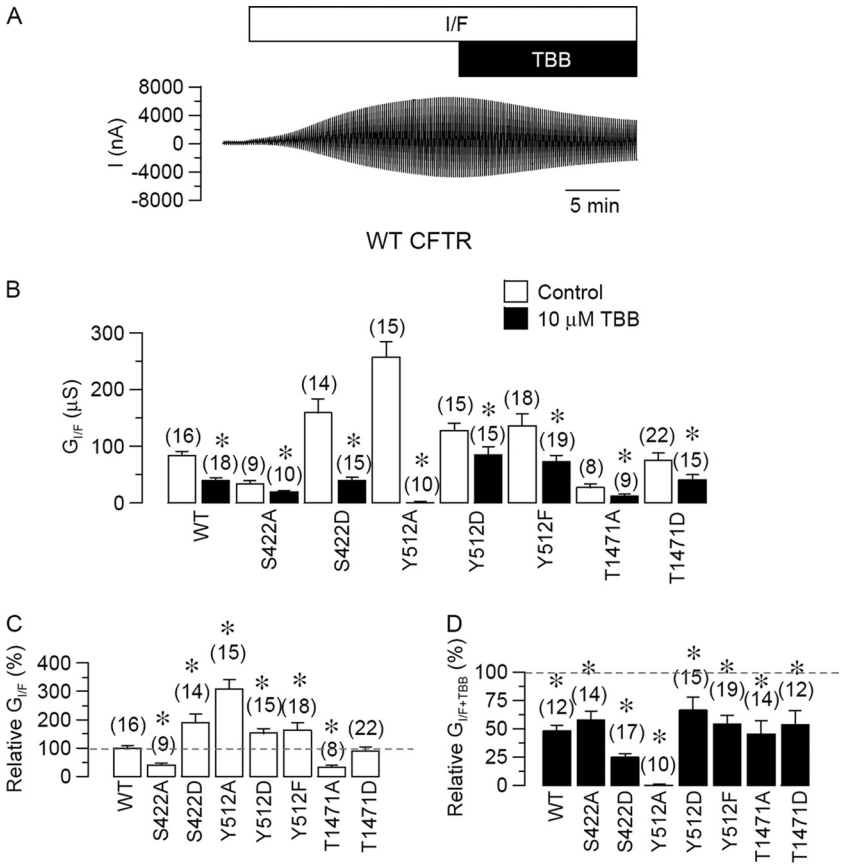

FIG. 5. Identification of functionally relevant CK2 sites in CFTR. (A) Whole-cell current measured in a wt-CFTR-expressing oocyte before and after activation by IBMX/forskolin (I/F; 1 mM/2 μM, respectively) and effects of the CK2 inhibitor TBB (10 μM). (B) Summary of the calculated IBMX/forskolin-activated whole-cell conductances for wt CFTR and CFTR mutants and whole-cell conductances in the presence of TBB. (C) Whole-cell conductances of CFTR mutants relative to wt CFTR. (D) TBB-inhibited whole-cell conductances of CFTR mutants relative to wt CFTR. Data indicate means ± standard errors of the means. Numbers in parentheses are numbers of experiments. Asterisks indicate significant inhibition by TBB (B) and significant difference from wt CFTR (unpaired *t* test and ANOVA) (C and D).

consensus sites for CK2 phosphorylation, a serine or threonine residue specified by an acidic side chain at position $n + 3$ (S/T-x-x-E/D/pS) (19), and found the presence of 21 putative CK2 phosphorylation sites in CFTR: S4, T360, T388, S422, T501, S511, T582, S605, T629, S678, T803, T816, T990, T1121, T1149, T1211, T1263, S1311, S1326, S1442, and T1471.

Based on their predicted functionality, we chose three specific sites to proceed with further analyses, namely, (i) S422, which was shown *in vitro* to be a CK2 phosphorylation site in purified wt NBD1 (26); (ii) S511, for being exposed on the surface of NBD1 very close to the site of the most common CF-causing mutation (F508del) and previously identified as important for CK2-dependent regulation of CFTR function as a channel (39); and (iii) T1471 in the vicinity of the C-terminal regulatory site for NHERF1 anchoring and membrane traffic (25).

We used site-directed mutagenesis to replace these specific sites in wt CFTR with either an alanine (A) or an aspartate (D). The resultant cDNAs were used to create stably expressing BHK cell lines. CFTR variants were analyzed by WB to assess the steady-state levels of the different variants (Fig. 3), which showed that mutation of S422 or S511 to either A or D does not affect the processing of CFTR at steady state, assessed by mature CFTR (band C) as a percentage of total CFTR, i.e., immature CFTR (band B) plus band C (Fig. 3B). However, a pronounced effect is observed for both T1471 variants, with the presence of T1471A decreasing significantly the processing of CFTR at steady state by around 25% and with T1471D completely abolishing the appearance of the fully glycosylated form (Fig. 3A and B, last lanes).

Turnover and processing of CFTR bearing S422, S511, and T1471 mutations. The effect of these mutations on the turnover and processing of CFTR was then studied by the metabolic pulse-chase approach (Fig. 4A, D, and G, respectively). Analysis of results for either S422 or S511 mutants (Fig. 4B and E, respectively) shows that neither the turnover rate of the immature form (band B) nor its efficiency of processing into the mature glycosylated form (band C) is altered (Fig. 4C and F, respectively). However, pulse-chase experiments performed for T1471A/D CFTR variants show that mutation of T1471 slightly increases the turnover of band B (Fig. 4H). Moreover, the presence of T1471A significantly decreases processing efficiency of CFTR and T1471D completely impairs the appearance of its fully glycosylated form (Fig. 4I has no data points for T1471D), which explains the findings in Fig. 3. For T1471D,

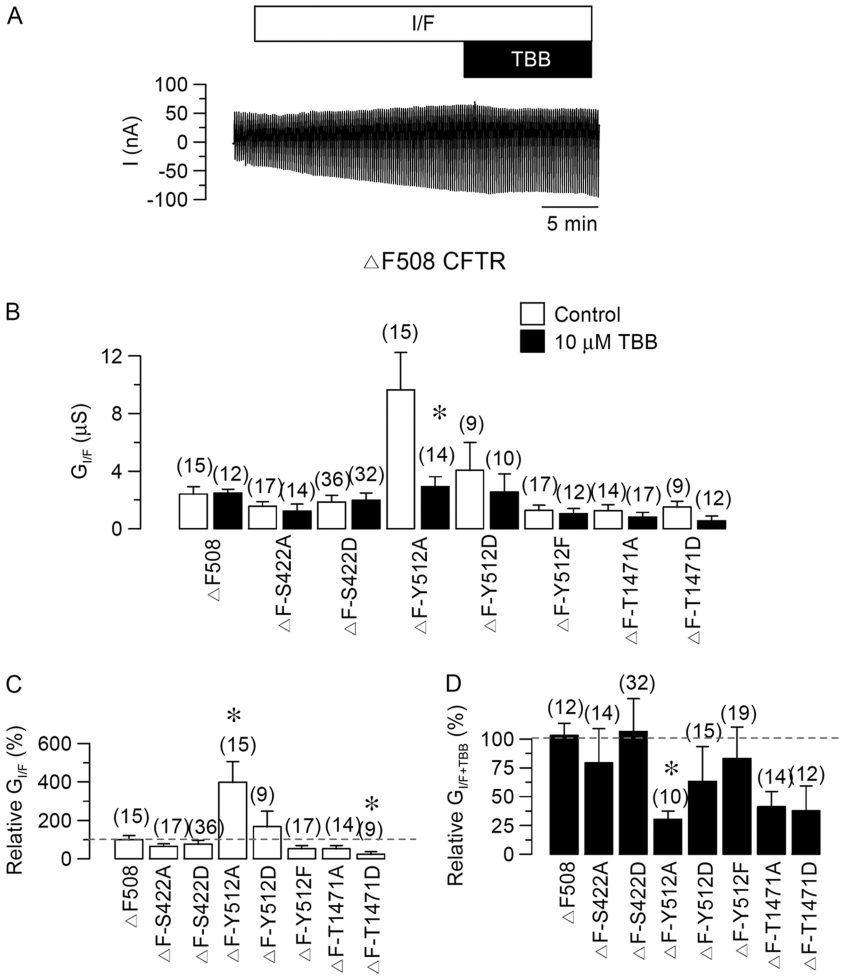

FIG. 6. CK2 regulation of F508del CFTR. (A) Whole-cell current measured in a F508del-CFTR-expressing oocyte before and after activation by IBMX/forskolin (1 mM/2 μM, respectively) and effects of the CK2 inhibitor TBB (10 μM). (B) Summary of the calculated IBMX/forskolin-activated whole-cell conductances for F508del CFTR and CFTR variants and whole-cell conductances in the presence of TBB. (C) Whole-cell conductances of CFTR variants relative to F508del CFTR. (D) TBB-inhibited whole-cell conductances of CFTR variants relative to F508del CFTR. Data indicate means ± standard errors of the means. Numbers in parentheses indicate numbers of experiments. Asterisks indicate significant inhibition by TBB (B) and significant difference from F508del CFTR (unpaired *t* test and ANOVA) (C and D).

we found a trend for faster disappearance of band B but a complete absence of band C.

Taken together, these results show that the CFTR S422 residue, although identified *in vitro* as a phosphorylation site for CK2, does not affect the trafficking of the protein in living cells. The same is observed for the S511 residue, which also appears not to be a critical spot for regulation of CFTR turnover and processing. In sharp contrast, the T1471 residue, previously described as a site for CFTR phosphorylation by CK2 (25), seems to be critical for CFTR turnover and processing.

Identification of functionally relevant CK2 sites in CFTR. We then characterized the functional effects of these CK2 site variants of CFTR upon channel conductance. First, we expressed wt CFTR in *Xenopus* oocytes and activated it by stimulation with IBMX (1 mM) and forskolin (2 μM) in the absence and in the presence of the CK2 inhibitor TBB (Fig. 5A).

Whole-cell currents that were measured in CFTR-expressing oocytes after stimulation with IBMX and forskolin were due to activation of wt CFTR. The baseline conductance of 4.6 ± 0.7 μS ($n = 15$) measured under control conditions was increased by I/F to 83 ± 7 μS and was reduced by 5 μM CFTRinh172 to 14.7 ± 3.7 μS. Calculation of the IBMX/forskolin-activated whole-cell conductance clearly indicated significant inhibition by TBB (Fig. 5B, bars 1 and 2) (by 53% ± 7%). Next, we expressed the CK2-phosphorylation CFTR mutants with mutations of S422 and T1471 to either alanines or aspartates, as well as the SYK-phosphorylation CFTR mutant Y512, to test whether the latter affects the phosphorylation of CFTR by CK2 (19). In *Xenopus* oocytes, all of these mutants produced significant whole-cell currents. While mock-transfected oocytes had a whole-cell conductance of 1.1 ± 0.2 μS ($n = 15$) under control conditions, which was marginally increased to 1.3 ± 0.3 μS ($n = 15$) after stimulation with IBMX and forskolin, oocytes expressing CFTR variants increased whole-cell conductances significantly.

Mutation of residues S422, Y512, and T1471 to either alanine or aspartate variably inhibited or augmented CFTR con-

ductance (Fig. 5B, normalized against wt control for ease of comparison in Fig. 5C and D). In particular, the TBB sensitivity of the inhibition of CFTR conductance was significantly reduced for S422A (Fig. 5B, bars 3 and 4) and Y512D (bars 9 and 10) but was augmented for S422D and almost doubled for Y512A (Fig. 5B). Rather impressive was the finding that such increased IBMX/forskolin-induced conductance was completely inhibited by TBB. These data indicate that apart from the formerly suggested S511 (39), these other sites within CFTR appear to be essential for regulation by CK2, especially the potential SYK site at Y512. We also observed a 50% higher conductance for S422D and a 50% reduction with the S422A mutant relative to wt CFTR (compare bar 5 with bars 3 and 1 in Fig. 5B and summary in Fig. 5C). This is consistent with an important role for S422 phosphorylation in increasing CFTR activity.

CK2 regulation of F508del CFTR. We further examined the effects of the alanine and aspartate variants in a F508del CFTR background.

Figure 6A shows a whole-cell current in F508del-CFTR-expressing and *Xenopus* oocytes. The whole-cell current and conductance are actually very small under control conditions (only 1.1 ± 0.2 μS; $n = 15$), indicating that there is no baseline Cl^- conductance in these oocytes. Stimulation with IBMX and forskolin only slightly, but significantly, activates an additional whole-cell current which increases the whole-cell conductance to 3.4 ± 0.6 μS ($n = 15$).

As reported earlier (39), we confirmed in F508del CFTR that this reduced whole-cell Cl^- conductance is insensitive to CK2 inhibition (Fig. 6A and B). None of the above mutations caused significant effects on either of the IBMX/forskolin-induced whole-cell currents on the F508del background, except for Y512A, which increased whole-cell currents significantly and was newly demonstrative of inhibition of the currents by TBB (Fig. 6B and D, bar 4). Notably, elimination of this SYK site in both wt CFTR and F508del CFTR additionally enhanced baseline Cl^- conductance in *Xenopus* oocytes in the absence of IBMX and forskolin (Fig. 7). This suggests that the phosphorylation status of CFTR at Y512 influences CFTR either by keeping the channel closed or by causing a reduction in CFTR cell surface expression, but independently of F508, as judged by the enhanced basal CFTR activity of both Y512A-wt CFTR and Y512A-F508del CFTR (Fig. 7A and B). Of note, however, the magnitude of the conductance for the Y512A-F508del CFTR variant was still small relative to wt CFTR.

Turnover and processing of CFTR bearing Y512 mutations. As mutation of Y512 in CFTR expressed in oocytes highlights a possible regulation of CFTR mediated by this residue, we next analyzed the effect of mutating this residue upon CFTR turnover and processing. As described above, mutations of Y512 to A, D, E, and additionally F (an aromatic residue of a size similar to tyrosine) were introduced into wt-CFTR-pNUT and the resulting vectors were used to generate stable BHK cells (Fig. 8A). These results show that steady-state levels of total CFTR are significantly affected by these variants, with the least effect being observed with replacement of phenylalanine by either tyrosine or glutamate (Fig. 8A, lanes 4 and 5). Processing of CFTR, however, is strongly affected by the Y512A,

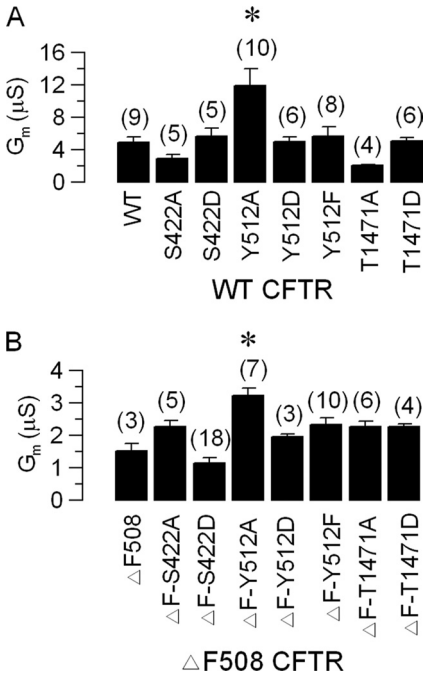

FIG. 7. Enhanced baseline CFTR activity by mutation of the SYK phosphorylation site. (A) Summary of the baseline whole-cell conductances (before stimulation with IBMX/forskolin) generated in oocytes expressing wt CFTR and CFTR mutants. (B) Summary of the baseline whole-cell conductances (before stimulation with IBMX/forskolin) generated in oocytes expressing F508del CFTR and various CFTR variants on an F508del background. Data indicate means ± standard errors of the means. Numbers in parentheses indicate numbers of experiments. Asterisks indicate significant difference from wt CFTR (ANOVA).

-D, and -E variants but not by the presence of phenylalanine residue (Fig. 8B).

The turnover and processing of these variants were also assessed by pulse-chase experiments. Results show that mutation of Y512 to an alanine or an aspartate significantly decreases the efficiency of processing of wt CFTR (Fig. 8E) without a significant impact upon the turnover of the immature form (Fig. 8D). The presence of the bulky side chain of phenylalanine (more comparable in size to that of tyrosine) or the longer negatively charged side chain of glutamate again does not affect the turnover of band B (Fig. 8G), and although decreasing significantly the efficiency of processing, this decline is less pronounced than that observed for Y512A or -D (compare Fig. 8H with Fig. 8E).

Levels of CFTR at the membrane are affected by Y512 mutations. In order to further explore the relevance of Y512 for CFTR trafficking, levels of CFTR at the membrane were assessed for these variants by cell surface biotinylation. Results show that replacement of Y512 by a negative residue (glutamate) decreases the plasma membrane levels of CFTR and that the replacement of Y512 by phenylalanine slightly increases the amount of membrane CFTR (Fig. 9).

SYK is an important regulator of CFTR. As studies with Y512 CFTR variants highlighted the relevance of this residue in the regulation of CFTR turnover, processing, and function, we further verified the role of SYK for activation of CFTR. For

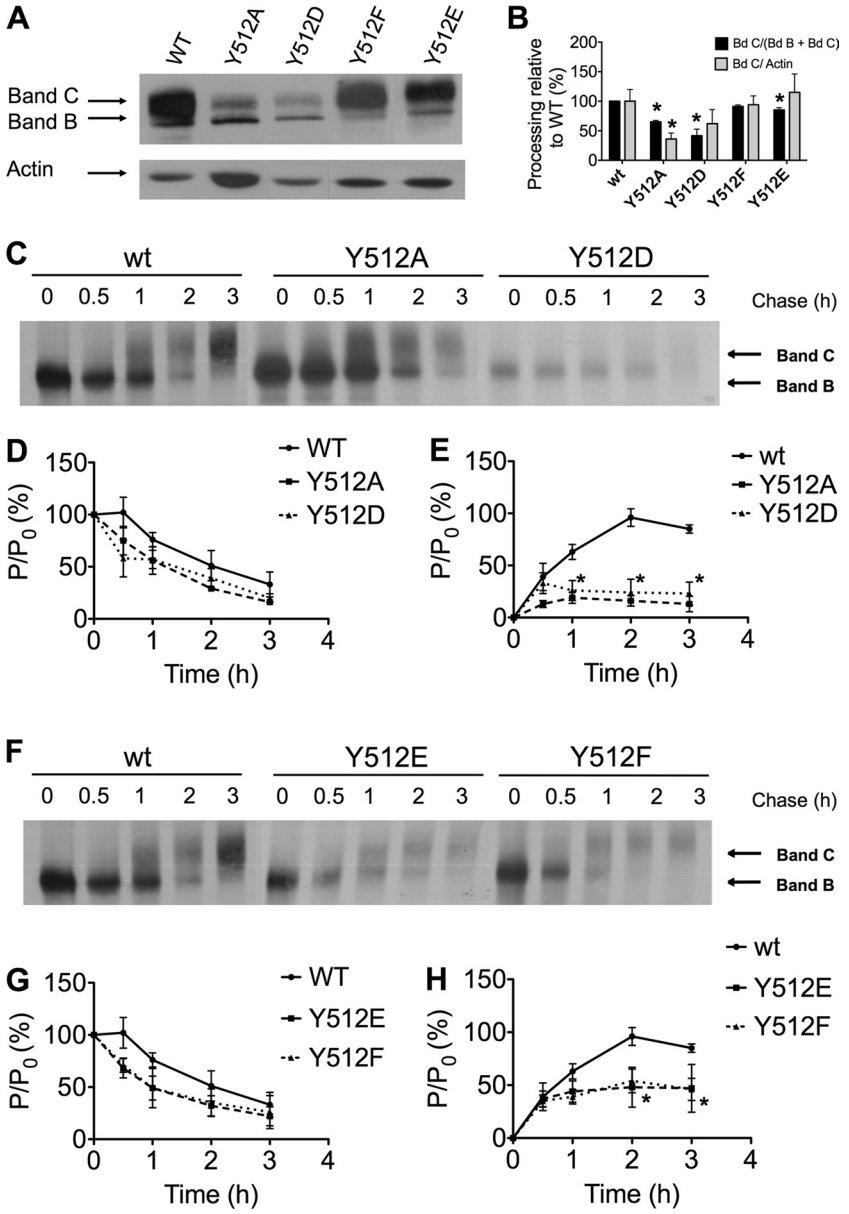

FIG. 8. Biochemical analysis of SYK phosphorylation site variants. (A) Steady-state levels of CFTR bearing Y512 mutations. WB of total protein (30 μg) from BHK cells stably expressing CFTR bearing different mutations. Actin was also assessed as a loading control. (B) Processing of CFTR at steady state was assessed by densitometry and shown as the ratio of band C to total CFTR (C/B+C), normalized to wt CFTR (black bars). Amount of mature band C CFTR was also assessed as ratio of band C to actin, again normalized to wt CFTR (grey bars). Asterisks indicate significant differences from wt CFTR (*t* test, $P < 0.05$). (C and F) BHK cells stably expressing wt, Y512A, Y512D, Y512E, or Y512F CFTR were analyzed by pulse-chase as in Fig. 2, followed by immunoprecipitation with anti-CFTR 596 Ab. (D, E, G, and H) Electrophoresis, fluorography, and quantification were also performed as in Fig. 2 but using the ImageQuant software to determine the turnover of the core-glycosylated form (band B) (D and G) and the efficiency of maturation (E and H). Images and quantitations are representative of a total of 3 to 4 experiments. Asterisks in panels E and H indicate differences from wt CFTR for the time points indicated (*t* test, $P < 0.05$).

this, we examined the effects of the SYK inhibitor 574711 (Calbiochem, Germany) on activation of wt CFTR and F508del CFTR in *Xenopus* oocytes. As shown in Fig. 10, 200 nM SYK inhibitor 574711 largely augmented the whole-cell currents produced by either wt CFTR or F508del CFTR in *Xenopus* oocytes (Fig. 10), to a degree similar to that observed for Y512A (Fig. 5B). Moreover, inhibition of SYK appears to sensitize CFTR for inhibition by TBB, judged by the near-complete post-TBB inhibition of CFTR for this variant (in Fig. 10, compare black bars with white ones, under SYK inhibitor). To investigate whether this sensitization is specific, we tested for a possible effect of another kinase site in the vicinity, namely, serine S519, a putative site for phosphorylation by Chk1. We thus tested the effect of Chk1 inhibitor 218078 (Calbiochem, Germany). After treatment with a 200 nM concentration of this inhibitor, we did not find any significant effects on wt CFTR conductance, while F508del CFTR conductance was reduced by inhibition of Chk1 (data not shown).

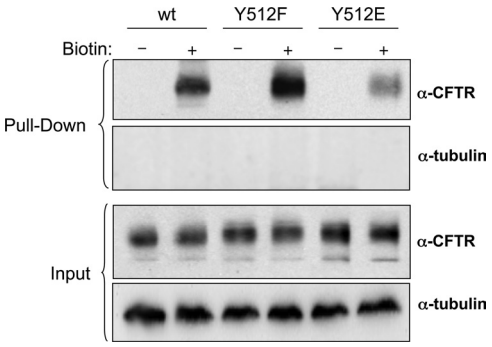

FIG. 9. Cell surface expression of CFTR variants. BHK cells stably expressing either wt, Y512F, or Y512E CFTR were subjected to surface protein biotinylation, followed by streptavidin pulldown. Shown are WB results for both pulled-down and input fractions, probed with anti-CFTR 596 monoclonal antibody. As controls for assay specificity, the intracellular protein α-tubulin was also stained, and nonbiotinylated samples (without biotin) were analyzed for each cell line. Blots shown are representative of three independent experiments.

SYK is expressed in respiratory cell lines and coprecipitates with CFTR. In order to assess the physiological relevance of these findings, we used reverse transcription-PCR (RT-PCR) to assess whether SYK is expressed in human nasal epithelial cells from CF patients (F508del homozygous) and controls as well as in three respiratory established cell lines, the submucosal gland cell line Calu-3 and a bronchial cell line homozygous for F508del (with no detectable endogenous expression of CFTR) virally transduced with either wt (CFBE-wt) or F508del CFTR (CFBE-F508del). We extracted RNA, applied RNase-free DNase digestion, and synthesized cDNA with random hexamers. This material was used as a template to amplify a 153-bp fragment with SYK-specific primers. The band observed in all the cDNA samples analyzed, but absent in the DNase-treated mRNA samples (Fig. 11A), confirmed the specific amplification of SYK, thus indicating that this kinase is expressed in all the tissues/cell lines tested (Fig. 11A).

Additionally, we assessed whether SYK precipitates *in vivo* with wt CFTR. CFBE cells stably expressing wt CFTR were used to immunoprecipitate CFTR under low-stringency conditions. Immunoprecipitated protein samples were then used to assess the presence of SYK by WB.

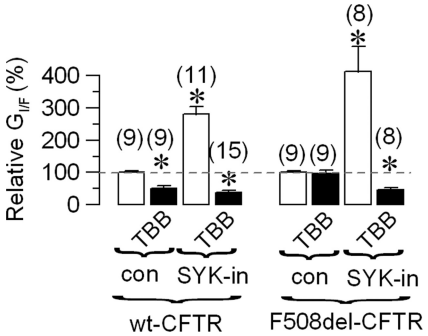

FIG. 10. Inhibition of SYK activates CFTR. Summary of the whole-cell conductances generated by wt CFTR (left) and F508del CFTR (right), measured in the absence or presence of TBB (10 μM) and the SYK inhibitor 574711 (200 nM), relative to the whole-cell conductances measured under control conditions. Data indicate means ± standard errors of the means. Numbers in parentheses indicate numbers of experiments. Asterisks indicate significant difference from control (unpaired *t* test and ANOVA).

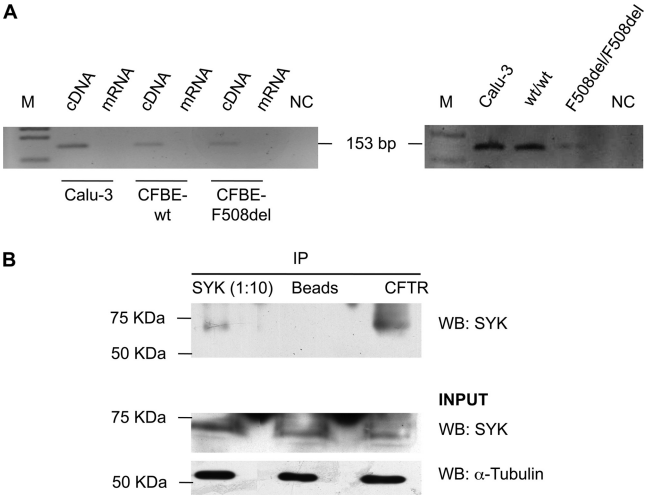

FIG. 11. SYK is expressed in human nasal cells and interacts with CFTR *in vivo*. (A) Expression of SYK mRNA in human nasal cells and in respiratory cell lines. (Left panel) Total RNA was extracted from the submucosal gland cell line Calu-3 (lanes 1 and 2) and from a bronchial cell line homozygous for F508del (and with no detectable endogenous expression of CFTR) transduced with either wt (lanes 3 and 4) or F508del (lanes 5 and 6) CFTR. RNA was subjected to digestion with RNase-free DNase. cDNA was synthesized using SuperScript II reverse transcriptase, and PCR with primers specific for SYK was performed in either cDNA (lanes 1, 3, and 5) or mRNA (lanes 2, 4, and 6) samples. (Right panel) Total RNA was extracted from human nasal epithelial cells obtained from a non-CF individual (lane 2) and a CF patient homozygous for F508del (lane 3). cDNA synthesis and PCR for SYK were performed as described above. Calu-3 cDNA was included as a positive control. Lane NC, PCR negative control. Lane M, ϕX174/HaeIII ladder. (B) CFTR forms complexes *in vivo* with SYK. CFTR was immunoprecipitated from CFBE-wt cells. The immunoprecipitated complex was blotted for SYK. As a positive control, SYK was detected by WB after immunoprecipitation (1:10 of the immunoprecipitate was loaded). As a negative control, pulldown was also performed with protein G-agarose beads and samples were blotted for SYK. Loading controls show equivalent amounts of SYK and α-tubulin in the precleared lysates (equivalent amounts were assessed).

Results show that, after CFTR immunoprecipitation, we were able to detect SYK and that the kinase is not pulled down in the bead control (Fig. 11B, upper panel). Data also show that in the human epithelial respiratory cell lines CFBE-wt and also Calu-3 (data not shown, confirmed $n = 3$), CFTR can interact with SYK.

SYK phosphorylates *in vitro* CFTR NBD1 at Y512. To further strengthen our findings, we then analyzed whether SYK is able to phosphorylate CFTR NBD1. To this end, purified recombinant NBD1 (rNBD1) and immunopurified YFP-SYK were used in an *in vitro* phosphorylation assay. Results show that besides catalyzing its autophosphorylation, SYK is also able to phosphorylate CFTR-NBD1 (Fig. 12).

A similar approach was also performed with Y512-mutated NBD1, and data show that mutation of this residue completely abolishes the phosphorylation of rSUMO-NBD1 or decreases the levels of phosphorylated Myc-NBD1 to those observed for the control in the absence of SYK, thus confirming that Y512 is the likely site for CFTR phosphorylation by SYK.

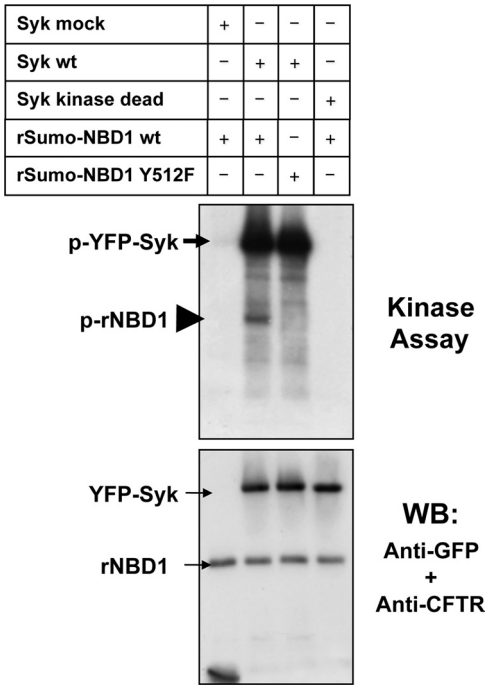

FIG. 12. *In vitro* phosphorylation of CFTR NBD1 by SYK. GFP control vector or full-length GFP-SYK wt or kinase dead was transfected into HEK293 cells, immunoprecipitated with anti-GFP antibodies using RIPA buffer, and then incubated *in vitro* with 1 μg recombinant Sumo-NBD1 wt or recombinant Sumo-NBD1 Y512F. WB results are shown to document successful protein precipitation and the presence of recombinant NBD1 (lower panels).

DISCUSSION

Regulation of CFTR by CK2. Our primary aim was to further characterize the role of CK2 in the regulation of CFTR traffic and function. We present further evidence that CK2-dependent regulation of CFTR has also a major role in electrolyte transport in native epithelial tissues (Fig. 1) and not only in cellular models.

Previous data, confirmed here (Fig. 6A), demonstrated that inhibition of CK2 correlates with reduced CFTR activity (39). Furthermore, here we show that this effect of pharmacological CK2 inhibition applies not only to CFTR function as a chloride channel but also to the processing of wt CFTR. Indeed, our results show that CK2 activity is also essential for the successful processing (and membrane trafficking) of CFTR: this may involve direct phosphorylation of CFTR by CK2, previously shown to occur at S422 (26), or this effect may involve other targets of CK2 that relate to CFTR-associated proteins.

Interestingly, the Na^+/H^+ exchanger 3 (NHE3) activity was also found to be inhibited by the structurally related CK2 inhibitor 2-dimethylamino-4,5,6,7-tetrabromo-1*H*-benzimidazole (DMAT). It was concluded that CK2 binds to the NHE3 C terminus and stimulates basal NHE3 activity by phosphorylating a separate single site on the NHE3 C terminus, which affects NHE3 trafficking (34). Space considerations precluded a more detailed analysis, but we note that CK2 also controls important CFTR interactors such as syntaxins that are also involved in CFTR processing to the plasma membrane (12).

Our analysis included the functional characterization of CK2 sites in CFTR that are involved in its regulation. Serine residue 422, previously identified not only as a consensus site but also as an actual site for phosphorylation of purified NBD1 by recombinant CK2, was shown here to be a critical residue, not for CFTR biogenesis, since neither turnover nor processing (Fig. 4A to C) is affected by a nonphosphomimic (S422A) or a phosphomimic (S422D), but for CFTR activity. Furthermore, although function of S422D CFTR is greatly affected by incubation with TBB, there is no change in its processing in the presence of this CK2 inhibitor (data not shown).

Functional assessment of these variants in *Xenopus* oocytes shows that S422A CFTR has reduced channel function and that S422D CFTR has increased function compared with wt CFTR (Fig. 5B and C). These results thus suggest that phosphorylation at S422 is involved in the regulation of CFTR function, contributing to its activation, consistent with its proposed pivotal position in the control of the interaction between NBD1 and NBD2 (16). In fact, we also observed an increased sensitivity to TBB for the S422D mutant and a decreased sensitivity for the S422A nonphosphorylatable mutant, suggesting that the introduction of a negative charge at serine 422 by CK2 as shown *in vivo* or by PKA (for which serine 422 is also a consensus site) (7) boosts CFTR sensitivity to CK2 activity, judged by the enhanced sensitivity to CK2 inhibition. Our data also suggest a role of residue S422 in modulating the binding of CK2 to the CFTR surface. The proposed role of this kinase as a multianchor protein partner responsible for the recruitment of other proteins to CFTR is evidenced here by the activating role of S422 (20).

The present study also provides further insight into the role of residues S511 and T1471. Serine 511 has been previously implicated in the regulation of CFTR by CK2, as the mutant S511D was found to be insensitive to TBB in *Xenopus* oocytes but to have no major impact on the single-channel behavior of CFTR (39). Our biochemical data show that this residue is in fact not critical for CFTR turnover and processing.

More striking, however, are the results for the T1471 variants. Indeed, data from mammalian cells show that this residue is critical for CFTR turnover and processing, significantly reducing (T1471A) or completely abolishing (T1471D) the appearance of mature CFTR. This residue is located very close to the C terminus of CFTR; thus, its substitution is probably affecting critical protein-protein interactions (e.g., with NHERF1) by further augmenting the negative charge in a region that is essential for CFTR trafficking at the plasma membrane (14). Strikingly, the patterns of maturation of F508del CFTR and T1471D are very similar in that neither of these variants results in a mature form of CFTR (band C). Moreover, we note the relative insensitivity of both variants to CK2 inhibition.

The fact that the quality control machinery is more leaky in *Xenopus* oocytes (8), where in fact CFTR anterograde trafficking seems to be preferred to the retrograde trafficking and endocytosis (38, 41), allowed us to characterize functionally these CFTR variants. The replacement of threonine T1471 by a noncharged residue reduces CFTR activity, while the additional negative charge does not affect the activity of CFTR. Overall results suggest that the T1471 mutation has a detrimental effect on the regulation of CFTR by CK2.

Results with T1471, although puzzling, highlight a dual role of putative CK2 sites in CFTR: potentiation of both CFTR processing and function but also possible regulation of its C-terminal specific interactions (which are critical for CFTR stability at the plasma membrane).

Taken together, our data on CFTR regulation by CK2 suggest opposing effects of residues S422 and T1471, with S422 having an activating role and T1471 having an inhibitory effect.

Regulation of CFTR by spleen tyrosine kinase. Another interesting finding of the present study was the regulation of CFTR by SYK, which is a crucial player in many biological functions, with important roles in hematopoietic cells and in the regulation of the inflammatory process (23). In our work, SYK was found to be expressed in cell lines expressing high levels of CFTR and also in material derived from either CF patients or healthy controls. Although expression of SYK in the airway epithelium has been described before (33) and its interaction with CFTR has been shown in BHK cells (21), we report here for the first time that it in fact interacts with CFTR in human epithelial respiratory cells.

As we confirmed that purified CFTR-wt-NBD1 is phosphorylated *in vitro* by SYK, likely at tyrosine 512, since it does not occur for CFTR-Y512F-NBD1, characterization of Y512 variants not only in *Xenopus* oocytes but also in stably transfected mammalian cells suggests that phosphorylation of CFTR by SYK may be involved in the regulation not only of CFTR membrane levels but also of CFTR activity. Furthermore, our functional data also show that phosphorylation of Y512 by SYK may affect the channel regulation by CK2—replacement of Y512 by a nonphosphomimic residue (Y512A) increases CFTR sensitivity to TBB, with the opposite being observed for Y512D.

These data are the first confirmation of this functional interaction between SYK and CK2. Previous observations evidenced that CK2 was able only to phosphorylate CFTR peptides corresponding to the sequence PGTIKENIIFGVSY$_{512}$D EYRYR, provided that residue Y512 was replaced with phosphotyrosine (26), strongly suggesting the potential for hierarchical phosphorylation, i.e., an interaction between CK2 and SYK at S511, the CK2 consensus, depending on a negative charge at the adjacent tyrosine (26, 27).

Our functional data also show that inhibition of SYK (or mutation of the potential SYK phosphorylation site) strongly augments Cl^- currents in oocytes, even those produced by F508del CFTR, confirming SYK as a novel target for pharmacotherapy of CF, as proposed by our recent study, where this effect was shown to be partially reversed by WNK4 (21). Interestingly, inhibition of SYK with small interfering RNA (siRNA) also downregulates proinflammatory molecules interleukin 6 (IL-6) and ICAM-1 (40), further reinforcing the relevance of SYK as a target to be knocked down for CF therapy. Moreover, phosphorylated SYK recruits and activates multiple downstream signaling molecules, including the small GTPases Rac1 and Cdc42 (13), the former of which was recently shown to play a role in CFTR trafficking and membrane anchoring (P. Matos and P. Jordan, personal communication).

Clarification of the role played by these two kinases in CFTR membrane trafficking and activity gives further insight into the complex regulation of the protein, potentially contributing to the discovery of new potential therapeutic targets for the treatment of patients with CF, here clearly favored, as kinase-based mechanisms are among those of higher "druggability."

ACKNOWLEDGMENTS

This work was supported by PTDC/BIA-BCM/112635/2009, PTDC/BIA-BCM/67058/2006, DFG SFB699 A6, and TargetScreen2 (EU-LSH-2005-1.2.5-3-037365). S.L., F.R., A.I.M., and M.S. are recipients of fellowships SFRH/BD/47445/2008, SFRH/BD/61883/2009, SFRH/BD/23001/2005, and SFRH/BD/35936/2007 (FCT, Portugal), respectively. A.M.'s laboratory is supported by the Wellcome Trust (069150/z/02/z).

A.M. thanks Kate Treharne for many useful insights.

REFERENCES

1. **Barro-Soria, R., R. Schreiber, and K. Kunzelmann.** 2008. Bestrophin 1 and 2 are components of the Ca(2+) activated Cl(−) conductance in mouse airways. Biochim. Biophys. Acta **1783:**1993–2000.
2. **Blom, N., T. Sicheritz-Ponten, R. Gupta, S. Gammeltoft, and S. Brunak.** 2004. Prediction of post-translational glycosylation and phosphorylation of proteins from the amino acid sequence. Proteomics **4:**1633–1649.
3. **Briel, M., R. Greger, and K. Kunzelmann.** 1998. Cl- transport by cystic fibrosis transmembrane conductance regulator (CFTR) contributes to the inhibition of epithelial Na+ channels (ENaCs) in Xenopus oocytes coexpressing CFTR and ENaC. J. Physiol. (Lond.) **508:**825–836.
4. **Chang, X. B., et al.** 1993. Protein kinase A (PKA) still activates CFTR chloride channel after mutagenesis of all 10 PKA consensus phosphorylation sites. J. Biol. Chem. **268:**11304–11311.
5. **Collins, F. S.** 1992. Cystic fibrosis: molecular biology and therapeutic implications. Science **256:**774–779.
6. **Cozza, G., et al.** 2009. Quinalizarin as a potent, selective and cell-permeable inhibitor of protein kinase CK2. Biochem. J. **421:**387–395.
7. **Csanady, L., K. W. Chan, A. C. Nairn, and D. C. Gadsby.** 2005. Functional roles of nonconserved structural segments in CFTR's NH2-terminal nucleotide binding domain. J. Gen. Physiol. **125:**43–55.
8. **Faria, D., et al.** 2011. Effect of Annexin A5 on CFTR: regulated traffic or scaffolding? Mol. Membr. Biol. **28:**14–29.
9. **Farinha, C. M., and M. D. Amaral.** 2005. Most F508del-CFTR is targeted to degradation at an early folding checkpoint and independently of calnexin. Mol. Cell. Biol. **25:**5242–5252.
10. **Farinha, C. M., P. Nogueira, F. Mendes, D. Penque, and M. D. Amaral.** 2002. The human DnaJ homologue (Hdj)-1/heat-shock protein (Hsp) 40 co-chaperone is required for the in vivo stabilization of the cystic fibrosis transmembrane conductance regulator by Hsp70. Biochem. J. **366:**797–806.
11. **Gentzsch, M., et al.** 2004. Endocytic trafficking routes of wild type and DeltaF508 cystic fibrosis transmembrane conductance regulator. Mol. Biol. Cell **15:**2684–2696.
12. **Gil, C., et al.** 2011. Protein kinase CK2 associates to lipid rafts and its pharmacological inhibition enhances neurotransmitter release. FEBS Lett. **585:**414–420.
13. **Greenberg, S.** 1999. Modular components of phagocytosis. J. Leukoc. Biol. **66:**712–717.
14. **Guggino, W. B., and B. A. Stanton.** 2006. New insights into cystic fibrosis: molecular switches that regulate CFTR. Nat. Rev. Mol. Cell Biol. **7:**426–436.
15. **Jensen, T. J., et al.** 1995. Multiple proteolytic systems, including the proteasome, contribute to CFTR processing. Cell **83:**129–135.
16. **Kanelis, V., R. P. Hudson, P. H. Thibodeau, P. J. Thomas, and J. D. Forman-Kay.** 2010. NMR evidence for differential phosphorylation-dependent interactions in WT and DeltaF508 CFTR. EMBO J. **29:**263–277.
17. **Lu, Y., et al.** 1998. Co- and posttranslational translocation mechanisms direct cystic fibrosis transmembrane conductance regulator N terminus transmembrane assembly. J. Biol. Chem. **273:**568–576.
18. **Meacham, G. C., et al.** 1999. The Hdj-2/Hsc70 chaperone pair facilitates early steps in CFTR biogenesis. EMBO J. **18:**1492–1505.
19. **Meggio, F., and L. A. Pinna.** 2003. One-thousand-and-one substrates of protein kinase CK2? FASEB J. **17:**349–368.
20. **Mehta, A.** 2007. The cystic fibrosis transmembrane recruiter the alter ego of CFTR as a multi-kinase anchor. Pflugers Arch. Eur. J. Physiol. **455:**215–221.
21. **Mendes, A. I., et al.** 2011. Antagonistic regulation of cystic fibrosis transmembrane conductance regulator cell surface expression by protein kinases WNK4 and spleen tyrosine kinase. Mol. Cell. Biol. **31:**4076–4086.
22. **Mense, M., et al.** 2006. In vivo phosphorylation of CFTR promotes formation of a nucleotide-binding domain heterodimer. EMBO J. **25:**4728–4739.
23. **Mocsai, A., J. Ruland, and V. L. Tybulewicz.** 2010. The SYK tyrosine kinase: a crucial player in diverse biological functions. Nat. Rev. Immunol. **10:**387–402.
24. **Navara, C. S.** 2004. The spleen tyrosine kinase (Syk) in human disease, implications for design of tyrosine kinase inhibitor based therapy. Curr. Pharm. Des. **10:**1739–1744.

25. **Ostedgaard, L. S., C. Randak, D. Vermeer, P. Karp, and M. J. Welsh.** 2006. CK2 phosphorylation influences transepithelial Cl- current in airway epithelia. Pediatr. Pulmonol. **43:**224.
26. **Pagano, M. A., et al.** 2008. Modulation of protein kinase CK2 activity by fragments of CFTR encompassing F508 may reflect functional links with cystic fibrosis pathogenesis. Biochemistry **47:**7925–7936.
27. **Pagano, M. A., et al.** 2010. Cystic fibrosis transmembrane regulator fragments with the Phe508 deletion exert a dual allosteric control over the master kinase CK2. Biochem. J. **426:**19–29.
28. **Peters, K. W., J. Qi, J. P. Johnson, S. C. Watkins, and R. A. Frizzell.** 2001. Role of snare proteins in CFTR and ENaC trafficking. Pflugers Arch. **443**(Suppl. 1)**:**S65–S69.
29. **Pissarra, L. S., et al.** 2008. Solubilizing mutations used to crystallize one CFTR domain attenuate the trafficking and channel defects caused by the major cystic fibrosis mutation. Chem. Biol. **15:**62–69.
30. **Riccaboni, M., I. Bianchi, and P. Petrillo.** 2010. Spleen tyrosine kinases: biology, therapeutic targets and drugs. Drug Discov. Today **15:**517–530.
31. **Riordan, J. R., et al.** 1989. Identification of the cystic fibrosis gene: cloning and characterization of complementary DNA. Science **245:**1066–1073. (Erratum, **245:**1437.)
32. **Roxo-Rosa, M., et al.** 2006. Revertant mutants G550E and 4RK rescue cystic fibrosis mutants in the first nucleotide-binding domain of CFTR by different mechanisms. Proc. Natl. Acad. Sci. U. S. A. **103:**17891–17896.
33. **Sanderson, M. P., C. W. Lau, A. Schnapp, and C. W. Chow.** 2009. Syk: a novel target for treatment of inflammation in lung disease. Inflamm. Allergy Drug Targets **8:**87–95.
34. **Sarker, R., et al.** 2008. Casein kinase 2 binds to the C terminus of Na+/H+ exchanger 3 (NHE3) and stimulates NHE3 basal activity by phosphorylating a separate site in NHE3. Mol. Biol. Cell **19:**3859–3870.
35. **Schultz, B. D., A. K. Singh, D. C. Devor, and R. J. Bridges.** 1999. Pharmacology of CFTR chloride channel activity. Physiol. Rev. **79:**S109–S144.
36. **Scott-Ward, T. S., and M. D. Amaral.** 2009. Deletion of Phe508 in the first nucleotide-binding domain of the cystic fibrosis transmembrane conductance regulator increases its affinity for the heat shock cognate 70 chaperone. FEBS J. **276:**7097–7109.
37. **Tabcharani, J. A., X. B. Chang, J. R. Riordan, and J. W. Hanrahan.** 1991. Phosphorylation-regulated Cl- channel in CHO cells stably expressing the cystic fibrosis gene. Nature **352:**628–631.
38. **Takahashi, A., S. C. Watkins, M. Howard, and R. A. Frizzell.** 1996. CFTR-dependent membrane insertion is linked to stimulation of the CFTR chloride conductance. Am. J. Physiol. **271:**C1887–C1894.
39. **Treharne, K. J., et al.** 2009. Inhibition of protein kinase CK2 closes the CFTR Cl channel, but has no effect on the cystic fibrosis mutant deltaF508-CFTR. Cell. Physiol. Biochem. **24:**347–360.
40. **Ulanova, M., et al.** 2005. Syk tyrosine kinase participates in beta1-integrin signaling and inflammatory responses in airway epithelial cells. Am. J. Physiol. Lung Cell. Mol. Physiol. **288:**L497–L507.
41. **Weber, W. M., et al.** 2001. Functional integrity of the vesicle transporting machinery is required for complete activation of cFTR expressed in Xenopus laevis oocytes. Pflugers Arch. **441:**850–859.
42. **Winter, M. C., and M. J. Welsh.** 1997. Stimulation of CFTR activity by its phosphorylated R domain. Nature **389:**294–296.